

C_{60} : the first one-component gel?

C. Patrick Royall

*School of Chemistry, University of Bristol, Bristol, BS8 1TS, UK**

Stephen R. Williams

Research School of Chemistry, Australian National University, Canberra, ACT 0200

Until now, gels have been formed of multicomponent soft matter systems, consisting of a solvent and one or more macromolecular or colloidal species. Here we show that, for sufficient quench rates, the Girifalco model of C_{60} can form gels which we identify by their slow dynamics and long-lived network structure. These gels are stable at room temperature, at least on the simulation timescale up to 100 ns. At moderate temperatures around 1000 K, below the bulk glass transition temperature, C_{60} exhibits crystallisation and phase separation proceeds without the dynamical arrest associated with gelation, in contrast to many colloidal systems.

PACS numbers:

I. INTRODUCTION

Gels form part of our everyday lives, yet are remarkably poorly defined. At moderate timescales, gels lack a clear distinction from ‘attractive glasses’ at high densities [1], while at low densities gels share many characteristics of liquids. Recently however, a distinction has been made between equilibrium and non-equilibrium gels [2]. The former are associated with systems whose intermolecular potential is not spherically symmetric, for example limited-valency models lead to equilibrium gels [3] and ‘empty liquids’ [4]. A second class of gels are formed through arrested metastable gas-liquid phase separation. In these ‘spinodal gels’ the metastable liquid phase is sufficiently dense to undergo dynamical arrest, suppressing demixing [5, 6], an extreme case of viscoelastic phase separation [7]. It was recently shown that the formation of clusters in this dense liquid phase prevents relaxation to the underlying crystal [8]. A third type of gel is formed through diffusion-limited cluster aggregation [9]. Other types of gels form in polymer solutions (spinodal gels), precipitate from solution, for example silica, and are formed by clays such as laponite, the nature of which remains disputed [10].

All these gels have one thing in common: they are multi-component systems, consisting of a solvent and at least one macromolecular or colloidal component. Although in equilibrium, the degrees of freedom of the solvent and smaller macromolecular/colloidal species can be formally integrated out, leading to a one-component treatment [11], it is important to note that consideration of an explicit solvent has recently been implicated in gelation, due to hydrodynamic interactions [12].

Here we enquire whether gels can be formed from a *single* molecular species. It has emerged from the colloid-polymer mixture literature [2, 13] that gels are associated

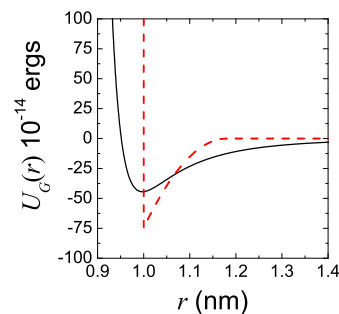


Figure 1: (color online) Interaction potentials. Solid black line, Girifalco potential used here to describe C_{60} [16]. Dashed red line, Asakura-Oosawa potential for colloid-polymer mixtures with a size ratio of 0.18 [8]. The Asakura-Oosawa parameters are scaled to aid comparison with the Girifalco potential.

with systems exhibiting a short-ranged attraction, compared to the particle/molecular diameter. Such systems also tend not to exhibit a stable liquid phase. Seeking a molecular system with such properties, one naturally turns to C_{60} . While it is not yet clear whether C_{60} has a stable liquid phase [14, 15], the commonly used model potential of Girifalco [1] [16], is understood to exhibit a liquid over a limited range in temperature [17]. The short-ranged attractions in C_{60} , relative to its molecular size, make it a most suitable candidate for one-component ‘spinodal gelation’. We shall thus pose the question: can C_{60} form a gel?

Before proceeding, let us be clear about what we mean by gelation in this paper. Certainly, gels are percolating networks. In the case of C_{60} , dynamical arrest will be required to prevent phase separation on the measurement timescale. To create such a spinodal gel, we shall therefore quench C_{60} into the region of the phase diagram where gas-liquid phase separation may form a bicontinuous spinodal-like texture and undergo dynamical arrest. By dynamical arrest, we require that the perco-

*Electronic address: paddy.royall@bristol.ac.uk

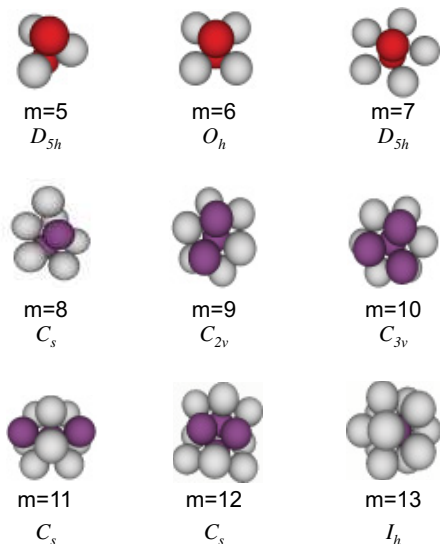


Figure 2: (color online) Ground state clusters for C_{60} [24]. Here the clusters are defined according to our topological cluster classification. C_{60} molecules are represented as spheres [19].

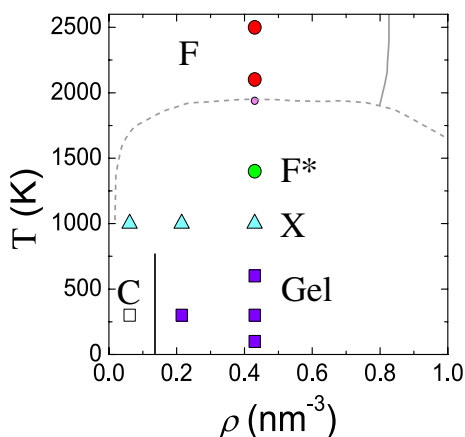


Figure 3: (color online) Phase diagram for C_{60} . Light dashed line is a guide to the eye denoting the liquid-gas binodal and solid line indicates freezing (from [17]). Percolation at low temperature is indicated by the solid black line. State points sampled with constant temperature simulations and corresponding structures are denoted as follows: (F) supercritical fluid, red circles; (F*) non-phase separated metastable fluid green circle; (X) phase-separated crystal, blue triangles; (C) isolated clusters, open square; gels, purple squares.

lating structure persists on the simulation timescale. Our requirement that phase separation is suppressed on the molecular lengthscale distinguishes our approach from materials such as fumed silica, which is formed from agglomerates of particles of condensed amorphous silica [18].

As in a previous study on a colloidal system [8], we shall characterise the structure in terms of clusters formed by small groups of C_{60} molecules in isolation. The

structures formed are then analysed in terms of topologies based on the minimum energy clusters using an algorithm we have recently developed for identifying clusters in condensed phases, the topological cluster classification (TCC) [19]. Clusters of C_{60} molecules have received considerable attention [20] and for small clusters the ground states are known both experimentally [20–23] and computationally [24]. Moreover, numerical studies have shown that for larger clusters C_{60} exhibits kinetic trapping, leading to a discrepancy between predicted ground state structures [24] and those observed experimentally below 500 K, which required annealing to access the ground state [22, 23].

We shall use molecular dynamics simulation to capture the behaviour of C_{60} on a timescale and system size sufficient that we may discuss gelation. For this purpose, we use the intermolecular interaction potential proposed by Girifalco [16], which reads

$$u(s) = \alpha_1 \left(\frac{1}{s(s-1)^3} + \frac{1}{s(s+1)^3} - \frac{2}{s^4} \right) + \alpha_2 \left(\frac{1}{s(s-1)^9} + \frac{1}{s(s+1)^9} - \frac{2}{s^{10}} \right) \quad (1)$$

where $s = r/2a$ and $2a = 7.1$ Angstroms, $\alpha_1 = 74.94 \times 10^{-15}$ erg, $\alpha_2 = 135.95 \times 10^{-18}$ erg. The Girifalco potential is plotted in 1. This Girifalco model is known to undergo dynamical arrest at high temperature and density [25–27]. The glass line intersects the gas-liquid spinodal at around $T_G \approx 1100$ K, while crystallisation is expected at higher temperature [25]. While locally crystalline structures still meet our criterion for gelation (ie a long-lived network), the absence of vitrification of the dense phase suggests that demixing may proceed. To prevent demixing, we need to quench below T_G . Noting that free surfaces enhance local diffusion [8, 28, 29], we expect that it will be necessary to quench well below T_G . This is consistent with experimental work where annealing to 610 K enabled small clusters to equilibrate [23]. Figure 1 also depicts the Asakura-Oosawa (AO) potential [30, 31] often used to describe colloid-polymer mixtures. The AO potential is plotted here to correspond to a polymer-colloid size ratio of 0.18 [8] which leads to a relative interaction range rather shorter than that of the Girifalco potential.

Our procedure is therefore as follows: we simulate Girifalco C_{60} at constant temperature, following an ‘instantaneous’ quench to enquire at what, if any, temperature, C_{60} forms a gel stable on the simulation timescale. We then perform quenches from high temperature to determine what quench rate is required to form gels.

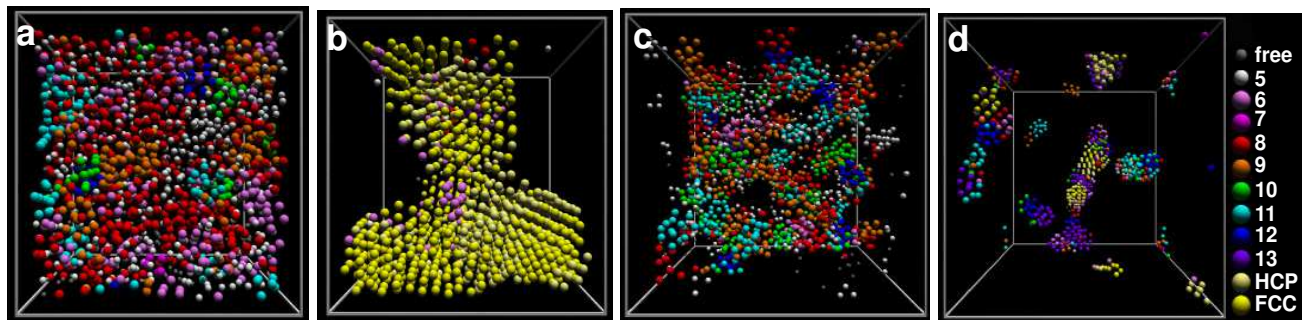


Figure 4: (color online) Typical (non-equilibrium) structures. (a) non-phase separated fluid ($\rho = 0.43 \text{ nm}^{-3}$, $T = 1400 \text{ K}$), (b) phase separated crystal ($\rho = 0.430 \text{ nm}^{-3}$, $T = 1000 \text{ K}$), (c) gel ($\rho = 0.215 \text{ nm}^{-3}$, $T = 300 \text{ K}$); (d) isolated clusters ($\rho = 0.108 \text{ nm}^{-3}$, $T = 300 \text{ K}$). All data shown here are from simulations at constant temperature. Colors denote the differing clusters or crystal structures to which the molecules belong, as shown on the right. Free denotes molecules not belonging to any clusters. Molecules are drawn around half actual size and represented as spheres.

II. SIMULATION DETAILS

A. Molecular dynamics simulation

We carry out simulations of two types. Constant temperature simulations, where the system is run up to 10^7 timesteps (99.6 ns) and sampled for a further 10^6 timesteps, and temperature quenches where temperature is decreased from 2328 K to 300 K at rates between 2.04×10^{11} and $2.04 \times 10^{13} \text{ Ks}^{-1}$. State points sampled for constant temperature simulations are shown in 3. Throughout we use molecular dynamics simulation with a Gaussian thermostat [32] with a timestep of 9.96 fs. We typically used 4000 or 2048 C₆₀ molecules. Runs with 4000 particles showed no qualitative differences. Occasionally, long times required smaller simulations of 864 particles. Data are shown after 9.96 ns of ‘equilibration’ or ‘aging’, unless otherwise stated. All simulations are performed at constant volume. We focus on data taken along the critical isochore $\rho \approx 0.43 \text{ nm}^{-3}$ unless otherwise stated. Results at lower density $\rho \approx 0.215 \text{ nm}^{-3}$ are qualitatively similar.

B. The topological cluster classification

To analyse the structure, we identify the bond network. Here we define two molecules as bonded if they approach within 1.23 nm, which is the approximate location of the first minimum of the pair correlation function $g(r)$ upon condensation. Having identified the bond network, we use the Topological Cluster Classification (TCC) to determine the nature of the cluster [19]. This analysis identifies all the shortest path three, four and five membered rings in the bond network. We use the TCC to identify structures of between 5 and 13 molecules which are topologically equivalent to ground states for the Girifalco potential (1) [24]. The clusters we identify are depicted in 2. In addition we identify the FCC and HCP thirteen particle structures in terms of a central particle and

its twelve nearest neighbours. For spherically symmetric potentials differing cluster structures are found as a function of interaction range [33]. For 11-membered clusters, our topological approach does not distinguish between C_s (11D in [33]) and C_{2v} (11C in [33]). Likewise for 12-membered clusters C_s (12C in [33]) and C_{5v} (12B in [33]) are identical for our purposes. For more details see [19]. If a molecule is found to be part of more than one cluster, we count it as the larger cluster. Moreover, if a molecule is found to be part of both a HCP and FCC local environment (for example in random close packed stacking), we count it as FCC.

III. RESULTS

A. Constant temperature simulations

We begin our presentation of the results by discussing our interpretation of the different structures we find. The equilibrium phase diagram is sketched in 3 [17] and typical structures are shown in 4. However, the system is not always able to fully equilibrate on the simulation timescale, a point to which we return below. For the densities we consider, at temperatures less than the triple point (around 1880 K [17]), equilibrium for the Girifalco model of C₆₀ is gas-crystal coexistence. However, for weak degrees of undercooling, crystal nucleation may not occur on the system sizes and timescales we consider, while for deep quenches, dynamical arrest limits access to equilibrium. In our simulations, these two non-equilibrium states are manifested as a metastable fluid, which can (but does not always) undergo phase separation prior to crystallisation, and a gel which forms a percolating network respectively. We identify these states by visual inspection of coordinate data and also require that more than 50% of molecules are in a locally HCP or FCC environment according to the TCC for any state point to be considered to be crystalline. We further require that gel states exhibit slow dynamics, in other words, that

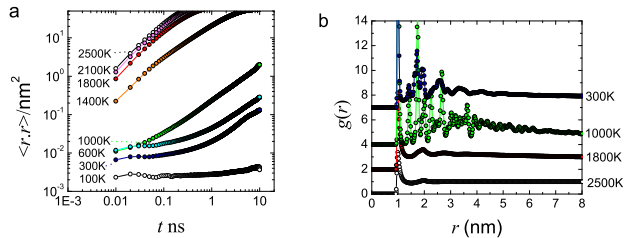


Figure 5: (color online) Mean squared displacement (a) and pair correlation functions (b) for constant temperature simulations. Here $\rho = 0.43$

nm^{-3} . In (b) the data are offset for clarity.

they do not phase separate or significantly coarsen on the simulation timescale.

More rigorous approaches, notably testing for percolation, have the disadvantage that for the system sizes we are able to tackle here, for $\rho \gtrsim 0.2 \text{ nm}^{-3}$, all state points were found to percolate according to our bonding criterion, despite the different structures evident in 4. At low density, isolated clusters were found [4(d)]. In our simulations, these clearly do not form a percolating network. Thus we sketch a percolation line in 3.

We have argued that in the case of C_{60} , gelation should be associated with slow dynamics. Plotting the mean squared displacement (MSD) at different temperatures in 5(a), we see a sharp fall in MSD between $T=1400$ and 1000 K . Thus we expect that, at 1000 K and below, we may find gelation. Inspection of the coordinate data in 4(b) shows that at 1000 K , C_{60} crystallises on our simulation timescales. This is consistent with nucleation studies carried out at higher density [34]. However at some of the lower temperatures we consider, it is clear C_{60} is sufficiently arrested that little restructuring is seen on the simulation timescale. Dynamically, therefore, it is possible that C_{60} can satisfy our requirements for classification as a gel. We note that these measures are performed on a system which is not in equilibrium for some state points. However, our intention here is to *qualitatively* demonstrate a substantial slowing of the dynamics.

Turning to local structural measures, namely the pair correlation function $g(r)$ we see three regimes in 5(b). At high temperatures, a fluid $g(r)$ is found. Note that even at temperatures below the triple point [17], we see little change in $g(r)$ on these simulation timescales. However, at lower temperatures (1000 K), the system crystallises. At lower temperatures still (300 K), although there is some local structure, overall the ordering is reduced. For temperatures less than around 1000 K $g(r)$ takes values substantially greater than unity at short range. This indicates density fluctuations on the lengthscale of a few particle diameters. While the limited size of our simulations preclude a definitive statement, we note that such local density fluctuations are indicative of networks, such as that found in 4(c).

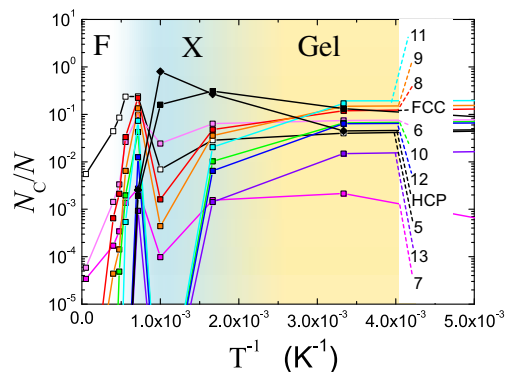


Figure 6: (color online) The population of molecules in ground state clusters of C_{60} as a function of inverse temperature. Here $\rho = 0.43 \text{ nm}^{-3}$. Shaded regions are a guide to the eye. Note the semi-log scale.

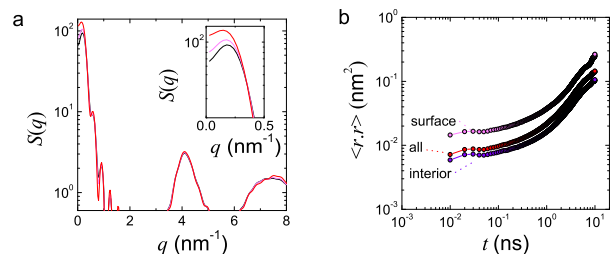


Figure 7: (color online) (a) Static structure factor $S(q)$ for gels at different ageing times t_w . Black line $t_w = 1 \text{ ns}$, pink line, $t_w = 10 \text{ ns}$, red line, $t_w = 100 \text{ ns}$. Inset shows first peak. $\rho = 0.21$

nm^{-3} $T = 300 \text{ K}$. (b) Mean squared displacement for surface (pink), and interior (purple) molecules. $\rho = 0.43 \text{ nm}^{-3}$ $T = 300 \text{ K}$.

Using the topological cluster classification, the same three regimes are identified, as shown in 6. At high temperatures ($T \gtrsim 1400 \text{ K}$), the population of all clusters rises sharply upon reducing the temperature. Around 1000 K , the structure is dominated by molecules in a locally crystalline environment, and the population of other clusters drops. At lower temperatures still, the population of locally FCC and HCP molecules drops, and the system is once again dominated by amorphous clusters. Of these, at 300 K , 11-membered C_s clusters are the most numerous, accounting for some 20% of the total population of C_{60} molecules. These clusters are five-fold symmetric, and it is tempting to infer that this five-fold symmetry might impede crystallisation [35]. The five-fold symmetric structure popularised by Frank [35], the 13-membered icosahedron is less popular than either HCP or FCC in this case, despite being the minimum energy cluster for 13 molecules [24]. We note that the icosahedron has been found to be relatively resistant to kinetic trapping [36] and is also observed experimentally [21].

We now consider the gel stability. Spinodal gels such

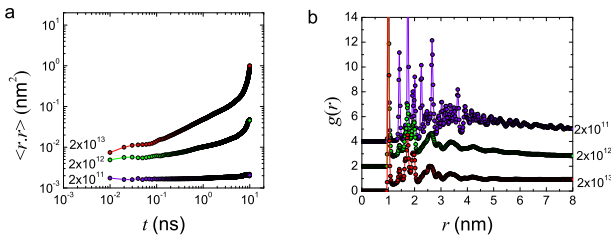


Figure 8: (color online) Mean squared displacement (a) and pair correlation functions (b) for quenches. Here $\rho = 0.43 \text{ nm}^{-3}$. Quench rate is denoted in Ks^{-1} .

as those we consider here are metastable to phase separation. Although that process is suppressed by slow dynamics induced by quenching, it is reasonable to pose the question, to what extent is phase separation effectively suppressed? To this end, we plot the static structure factor $S(q)$ in Fig. 7(a). Indeed a small degree of structural evolution is found, as shown by the slight shift in the first peak of $S(q)$. While this indicates some degree of coarsening, it is very clear that the gel lifetime exceeds the simulation timescale, noting that here the simulations are run for up to 100 ns.

Nevertheless, there is some degree of coarsening. We investigate possible coarsening mechanisms by considering the mean squared displacement of particles on the surface and in the interior of the ‘arms’ of the gel. We define molecules on the surface as those with fewer than eight neighbours. The analysis in Fig. 7(b) shows that indeed, molecules on the surface have a marginally higher mobility than those in the interior. This is qualitatively consistent with previous studies of gelation in colloidal systems [8, 29].

B. Temperature quenches

The picture that emerges from our analysis of the constant temperature runs is that at $T \lesssim 600 \text{ K}$, C_{60} can form gels, according to our criteria. However such ‘instantaneous quenches’ are unphysical for molecular systems (although essentially accessible to soft matter systems such as colloids). We therefore enquire as to what quench rate is required to form a gel. We choose to quench from a supercritical fluid at 2328 K to 300 K . Inspection of the phase diagram suggests that, for sufficiently slow quench rates, we might expect phase separation to occur in temperature regime $1940 \text{ K} \gtrsim T \gtrsim 600 \text{ K}$, and that crystallisation may also occur.

We thus consider a range of quench rates, and identify the final state as before. Data are presented for the 9.96 ns immediately following the quench. Mean squared displacement data [8(a)] shows that the quenches we have performed result in a state with relatively slow dynamics. Mobility is strongly suppressed for slower quench rates.

The pair correlation function data in 8(b) show a similar structural transitions to the constant temperature data, although here the transition occurs as a function of quench rate. For quench rates at or above $2.04 \times 10^{12} \text{ Ks}^{-1}$, we find that the $g(r)$ remains amorphous. A slower quench rate of $2.04 \times 10^{11} \text{ Ks}^{-1}$ results in a crystalline structure, which undergoes phase separation, similar to 4(b).

This observation is confirmed with the TCC analysis, where we consider the cluster populations in the quenched systems. In 9(a) we show average cluster populations for runs of 9.96 ns following the quench, and find a clear shift to a crystal-dominated structure for the slowest quench rate. In fact the trend towards a higher degree of crystallinity is apparent between the higher quench rates of 2.04×10^{13} and $2.04 \times 10^{12} \text{ Ks}^{-1}$. Turning to the mean squared displacement data in 8(a) we note that for rapid quenching in particular, some movement persists. In other words, the gel undergoes aging. Restructuring associated with this aging is apparent in the larger error bars for the $2.04 \times 10^{13} \text{ Ks}^{-1}$ quench rate in 9(a). In 9(b) we consider the local structural consequences of this aging. The data shows a gradual trend of increasing HCP and FCC local structures and a decrease of the most popular cluster, $m = 11 \text{ C}_{2v}$. This increase in crystallinity is consistent with previous studies on aging colloidal gels [37].

IV. DISCUSSION AND CONCLUSIONS

We begin the discussion by considering how practically realisable the C_{60} gels we have predicted might be. We have shown that gels form and exist on a simulation timescale of 10 ns. This leads to two main questions: firstly, can the gels form in the first place and secondly, how long can they last? Evidence from experimental work on clusters of C_{60} molecules suggests that in fact, long-lived metastable states are possible. Below around 500 K, clusters show little preference for ground states [20, 22, 23]. We thus argue that C_{60} can be prevented from equilibrating on an experimental timescale at room temperature, although we note that some aging can be seen in our simulations. The first question is potentially more challenging. The quench rates we have used are not currently experimentally feasible (maximum quench rates are around 10^6 Ks^{-1} by vapor deposition). Our predictions are that C_{60} will phase separate to crystal-gas coexistence on such a timescale. However, shear could be used to prevent crystallisation during quenching, allowing milder quench rates. Other possibilities include compressing low-temperature amorphous clusters. We note in 4(d) that the isolated clusters formed at $T = 300 \text{ K}$ are far from spherical and might reasonably be expected to form a gel upon increasing the density. Following [36] we also note that the Girifalco potential is not the only model for C_{60} . The Pacheco-Prates-Ramalho model [38] is in fact more sticky (shorter ranged) than that of Giri-

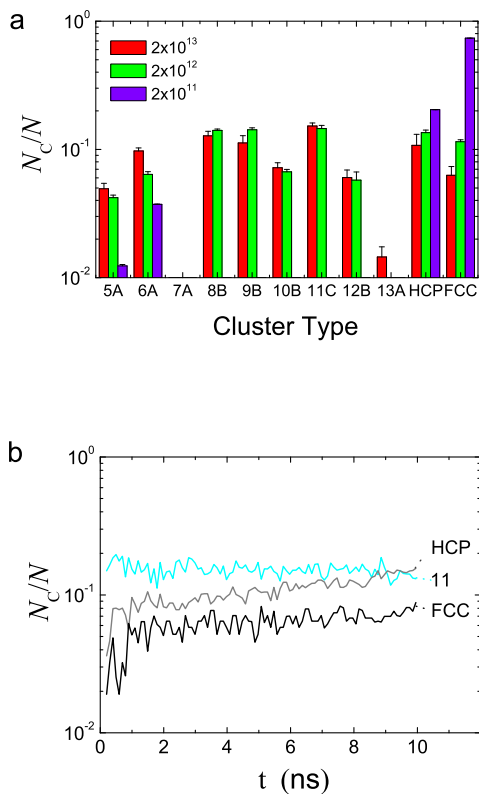


Figure 9: (color online) The population of molecules in ground state clusters of C_{60} for different quench rates (a). Quench rates are denoted in Ks^{-1} . (b) Structural changes upon aging in a gel formed after a quench rate of $2.04 \times 10^{13} Ks^{-1}$. Here $\rho = 0.43 \text{ nm}^{-3}$.

falco, which would be expected to promote gelation.

Another approach to producing one-component gels might be to consider larger fullerenes whose dynamics will be much slower. Such a candidate is C_{540} which may also exhibit a molecular shape with high symmetry and stability [39], although its high binding energy would necessitate quenching from very high temperatures at which thermal stability of the fullerene molecule may become a problem. The same might even hold for C_{60} whose thermal stability at high temperatures (such as criticality) is

disputed [40, 41], although at temperatures below 1700 K C_{60} is likely stable, so compressing disordered clusters remains a potential experimental route to forming gels of C_{60} .

The behaviour exhibited by C_{60} in the constant temperature simulations may be compared with that observed in colloidal suspensions, where interactions may be tuned [13], and which typically undergo ‘instantaneous’ quenching, due to the slow relaxation time of the mesoscopic colloidal particles. The main difference between the results presented here and those from a previous study on a colloidal gel [8] are that C_{60} exhibits a regime of crystallisation, which is almost entirely absent from the colloidal system, where the crystal-like local structures accounted for no more than one particle in 1000. There are at least three possible reasons for this difference. The first is that the relative interaction range is substantially longer in the case of C_{60} and this may facilitate crystallisation (see 1). Secondly, colloids are polydisperse, which might suppress, although should not prevent, crystallisation [42, 43]. Finally, we have used Newtonian dynamics for C_{60} while colloids are diffusive, although we are unaware of any studies considering the role of dynamics in crystallisation. In colloid simulation work with Brownian dynamics [44] with parameters comparable to experiments [8] there is some evidence that crystallisation can occur on the low temperature side of the metastable gas-liquid binodal in a monodisperse system. This suggests that the role of polydispersity in the colloid experiments may be important in suppressing crystallisation.

In summary, we have presented numerical evidence that C_{60} , under the right conditions can form a gel, which forms through arrested spinodal decomposition. Potentially, therefore, one-component gels might be realised. Whether these conditions are experimentally accessible remains an open question.

Acknowledgments

CPR acknowledges the Royal Society for financial support. The authors would like to thank Hajime Tanaka for many helpful discussions on the nature of the gel state, with particular reference to Laponite.

-
- [1] Zaccarelli, E.; Poon, W. C. K. *Proc. Nat. Acad. Sci.* **2009**, *106*, 15203–15208.
 - [2] Zaccarelli, E. *J. Phys.: Condens. Matter* **2007**, *19*, 323101.
 - [3] Del Gado, E.; Kob, W. *Europhys. Lett.* **2005**, *72*, 1032–1038.
 - [4] Bianchi, E.; Largo, J.; Tartaglia, P.; Zaccarelli, E.; Sciortino, F. *Phys. Rev. Lett.* **2006**, *97*, 168301.
 - [5] Verhaegh, N. A. M.; Asnaghi, D.; Lekkerkerker, H. N. W.; Giglio, M.; Cipolletti, L. *Physica A* **1997**, *242*, 104–118.
 - [6] Lu, P. J.; Zaccarelli, E.; Ciulla, F.; Schofield, A. B.; Sciortino, F.; Weitz, D. A. *Nature* **2008**, *435*, 499–504.
 - [7] Tanaka, H. *J. Phys.: Condens. Matter* **2000**, *12*, R207–R264.
 - [8] Royall, C. P.; Williams, S. R.; Ohtsuka, T.; Tanaka, H. *Nature Mater.* **2008**, *7*, 556–561.
 - [9] Allain, C.; Wafra, M. *Phys. Rev. Lett.* **1995**, *74*, 1478–1481.
 - [10] Jabbari-Farouji, S.; Tanaka, H.; Wegdam, G. H.; Bonn, D. *Phys. Rev. E* **2008**, *78*, 061405.

- [11] Likos, C. *Physics Reports* **2001**, *348*, 267–439.
- [12] Furukawa, A.; Tanaka, H. *Phys. Rev. Lett.* **2010**, *104*, 245702.
- [13] Poon, W. C. K. *Journal of Physics, Condensed Matter* **2002**, *14*, R859–R880.
- [14] Cheng, A.; Klein, M. L.; Caccamo, C. *Phys. Rev. Lett.* **1993**, *71*, 1200–1203.
- [15] Hagen, M. H. J.; Meijer, E. J.; Mooij, G. C. A. M.; Frenkel, D.; Lekkerkerker, H. N. W. *Nature* **1993**, *365*, 425–426.
- [16] Girifalco, L. A. *J. Phys. Chem.* **1992**, *96*, 858–861.
- [17] Costa, D.; Pellicane, G.; Abramo, M. C.; Caccamo, C. *J. Chem. Phys.* **2003**, *118*, 304–310.
- [18] Ihler, R. K. *The Chemistry of Silica*; Wiley and Sons Inc., New York, 1979.
- [19] Williams, S. R. *Cond.Mat.ArXiv* **2007**, *ArXiv:0705.0203v1*.
- [20] Baletto, F.; Ferrando, R. *Rev. Mod. Phys.* **2005**, *77*, 371–423.
- [21] Martin, T. P.; Naher, U.; Schaber, H.; Zimmermann, U. *Phys. Rev. Lett.* **1993**, *70*, 3072.
- [22] Branz, W.; Malinowski, N.; Schaber, H.; Martin, T. *Chem. Phys. Lett.* **2000**, *328*, 245–250.
- [23] Branz, W.; Malinowski, N.; Enders, A.; Martin, T. P. *Phys. Rev.* **2002**, *66*, 094107.
- [24] Doye, J. P. K.; Wales, D. J. *Chem. Phys. Lett.* **1996**, *262*, 167–174.
- [25] Abramo, M. C.; Caccamo, C.; Costa, D.; Ruberto, R. *J. Phys. Chem. B.* **2004**, *109*, 24077–24084.
- [26] Greenall, M. J.; Voightmann, T. *J. Chem. Phys.* **2006**, *125*, 194511.
- [27] Costa, D.; Ruberto, R.; Sciortino, F.; Abramo, M. C.; Caccamo, C. *J. Phys. Chem. B.* **2007**, *111*, 10759–10764.
- [28] Fakhraai, Z.; Forrest, J. A. *Science* **2009**, *319*, 600–604.
- [29] Puertas, A. M.; Fuchs, M.; Cates, M. E. *J. Chem. Phys.* **2004**, *121*, 2813–2822.
- [30] Asakura, S.; Oosawa, F. *J Chem Phys* **1954**, *22*, 1255–1256.
- [31] Vrij, A. *Pure Appl. Chem.* **1976**, *48*, 471–483.
- [32] Evans, D. J.; Morriss, G. *Statistical Mechanics of Nonequilibrium Liquids, 2nd Ed.*; Cambridge University Press, 2008.
- [33] Doye, J. P. K.; Wales, D. J.; Berry, R. S. *J. Chem. Phys.* **1995**, *103*, 4234–4249.
- [34] Ngale, K. N.; Desgranges, C.; Delhommelle, J. *J. Chem. Phys.* **2009**, *131*, 244515.
- [35] Frank, F. C. *Proc. R. Soc. Lond. A.* **1952**, *215*, 43–46.
- [36] Baletto, F.; Doye, J. P. K.; Ferrando, R. *Phys. Rev. Lett.* **2002**, *88*, 075503.
- [37] d’Arjuzon, R. J. M.; Frith, W.; Melrose, J. R. *Phys. Rev. E.* **2003**, *67*, 061404.
- [38] Pacheco, J. M.; Prates Ramalho, J. P. *Phys. Rev. Lett.* **1997**, *79*, 3873–3876.
- [39] Scuseria, G. E. *The equilibrium structures of giant fullerenes: faceted or spherical shape? An ab initio Hartree-Fock study of icosahedral C₂₄₀ and C₅₄₀* **1995**, *243*, 193–198.
- [40] Kolodney, E.; Tsipinyuk, B.; Budrevich, A. *J. Chem. Phys.* **1994**, *100*, 8542–8545.
- [41] Sommer, T.; Kruse, T.; Roth, P. *J. Phys. B.* **1996**, *29*, 4955–4964.
- [42] Moriguchi, I.; Kawasaki, K.; Kawakatsu, T. *J. Phys. II (France)* **1995**, *5*, 143.
- [43] Williams, S. R.; Snook, I. K.; van Megen, W. *Phys. Rev. E* **2001**, *64*, 021506.
- [44] Fortini, A.; Sanz, E.; Dijkstra, M. *Phys. Rev. E* **2008**, *78*, 041402.